Control of Grid Connected PMSG-Based Wind Turbine System with Back-To-Back Converter Topology Using Resonant Controller

Fekkak Bouazza, Menaa Mohamed, Loukriz Abdelhamid, Krim Mohamed L.

Abstract—This paper presents modeling and control strategy for the grid connected wind turbine system based on Permanent Magnet Synchronous Generator (PMSG). The considered system is based on back-to-back converter topology. The Grid Side Converter (GSC) achieves the DC bus voltage control and unity power factor. The Machine Side Converter (MSC) assures the PMSG speed control. The PMSG is used as a variable speed generator and connected directly to the turbine without gearbox. The pitch angle control is not either considered in this study. Further, Optimal Tip Speed Ratio (OTSR) based MPPT control strategy is used to ensure the most energy efficiency whatever the wind speed variations. A filter (L) is put between the GSC and the grid to reduce current ripple and to improve the injected power quality. The proposed grid connected wind system is built under MATLAB/Simulink environment. The simulation results show the feasibility of the proposed topology and performance of its control strategies.

Keywords—Wind, grid, PMSG, MPPT, OTSR.

I. INTRODUCTION

THE wind is a clean, free, and readily available renewable energy source. This later has become more and more one of the faster growing and clean energy resources [1], [2]. It is essentially based on fixed and variable wind speed turbines. However, the fixed wind speed turbines are limited because the wind power is not fully exploited. While, the variable wind speed turbines have many advantages. Indeed, besides they can operate at Maximum Power Point (MPP) over a wide range of wind speeds, it presents a reduced mechanical stresses and greater output power compared to the fixed wind speed turbines [1], 82]. Also, since a direct-in-line system can operate at low speeds, the gearbox can be omitted. Further, this direct-driven PMSG is suitable for the wind system applications due to its high power and high torque, which means a high efficiency. Moreover, by using PMSG, the DC excitation system is eliminated and allows reducing weight, losses, costs, and maintenance requirements (no slip rings are required). Consequently, the use of a PMSG with gearless

B.Fekkak is PhD student with the Power Electronics and Industrial Systems Laboratory, Department of Electrical Engineering, University of Sciences and Technology Houari Boumediene, Algeria (corresponding author, phone: +213770997093; e-mail: bfekkak@ usthb.dz).

M.Menaa is professor with the Power Electronics and Industrial Systems Laboratory, Department of Electrical Engineering, USTHB, Algeria (e-mail: mmenaa@ usthb.dz).

A.Loukriz was with Polytechnic School of Algiers, Algeria (e-mail: abdelhamid.loukriz@g.enp.edu.dz).

L. Krim was with the Economic Department, University of Medea, (e-mail: krimmohamedlamine999 @gmail.com).

construction represents an efficient and robust solution that should be beneficial especially for offshore applications, where reduced maintenance is essential [3]. Also, and due to the intensified grid codes around the world, direct-driven PMSG wind turbine systems could be favored in the future over the DFIG wind turbine [4]. The pitch angle transformation is not either considered in this paper, since the studied system is chosen to operate between the cut-in and the rated wind speed [5], [6]. Furthermore, applications of Power Electronics Converters (PECs) in the field of power systems are making a great impact for power conditioning especially in renewable energy systems integrated to the electrical grid. In fact, the configuration of PMSG Wind Energy Conversion Systems (WECSs) based on back-to-back converters is the most attractive in the case of Distributed Power Generators (DPGs) [7]. The impact of the back-to-back converters is more reliable and allows easy synchronizing of the renewable energy sources with the grid.

The design of the back-to-back based PECs is widely classified as Voltage Source Converters (VSC) and current source converters (CSC) [8]. Both have their own advantages and disadvantages, in fact they depend on the requirement of the system. Researchers according to the research context choose the converter source type and design configuration. However, the main advantages of these models remain that they are both controllable, even their control strategy is complex and expensive due to the need of IGBT-based PECs.

In our case, Back-to-Back AC/DC/AC PECs based on 12 pulses are used. Furthermore the modeling and behavioral simulation of PMSG-based small power generation connected to the grid is proposed. The studied system, which is presented in Fig. 1, includes: wind turbine with rated power (20 kW) connected to a PMSG without speed multiplier. The vector oriented control strategy is used for the GSC in order to realize concept of the decoupled current control. This is useful for simultaneously and independently controlling active and reactive power, and for maintaining a constant DC bus voltage [9]-[12]. The Field Oriented Control (FOC) is used for the MSC to command the PMSG speed [11]. Furthermore, the simulation model of small and medium-sized PMSG system is built under MATLAB/Simulink. Each module parameter is calculated accurately.

The simulation results show the control strategy performance of the small and medium-sized PMSG in power generation. They also demonstrate that such system based on back to back topology is very advantageous.

World Academy of Science, Engineering and Technology
International Journal of Mechanical and Mechatronics Engineering
Vol:14, No:5, 2020

II. WIND ENERGY SYSTEM MODEL

WECS considered in this work is shown in Fig. 1 [13], [14]. It includes the wind turbine, a PMSG and back-to-back based PECs. Back-to-back bidirectional converters feed the stator. This wind system is connected to the grid via the Point of Common Collecting (PCC). This system allows conversion of the wind energy into mechanical energy through wind turbine. This mechanical energy is transformed in electrical energy by the means of a PMSG, a PECs and a filter (L) into the electrical grid.
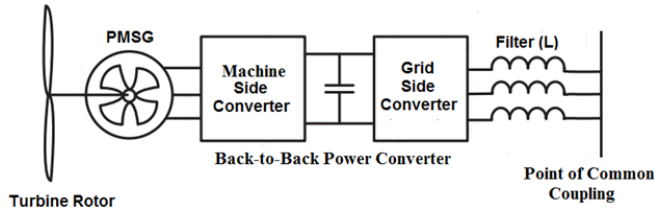

Fig. 1 WECS based on PMSG

A. Wind Turbine Model

The theoretical power applied to the wind turbine is given by (1) [13], where ρ is the density of the air, R is the radius of the surface swept by the turbine blades, v is the wind speed in meters per second, λ is the Tip speed ratio (TSR) given by (2) and C_p is the power coefficient (3):

$$P_t = \frac{1}{2}.\rho.\pi.R^2.v^3.C_p(\lambda) \tag{1}$$

where

$$\lambda = \frac{\omega_m.R}{v} \tag{2}$$

ω_m is the blades angular velocity

$$C_p(\lambda) = 0.22.\left(\frac{116}{\lambda_i} - 5\right).exp^{\frac{-12.5}{\lambda_i}} \tag{3}$$

where:

$$\lambda_i = \frac{1}{\frac{1}{\lambda} - 0.035} \tag{4}$$

Further, the Mechanical torque (T_t) presented in (5), can be deduced form (1):

$$T_t = \frac{P_t}{\omega_m} = \frac{1}{2\lambda}.\rho.\pi.R^3.v^2.C_p(\lambda) \tag{5}$$

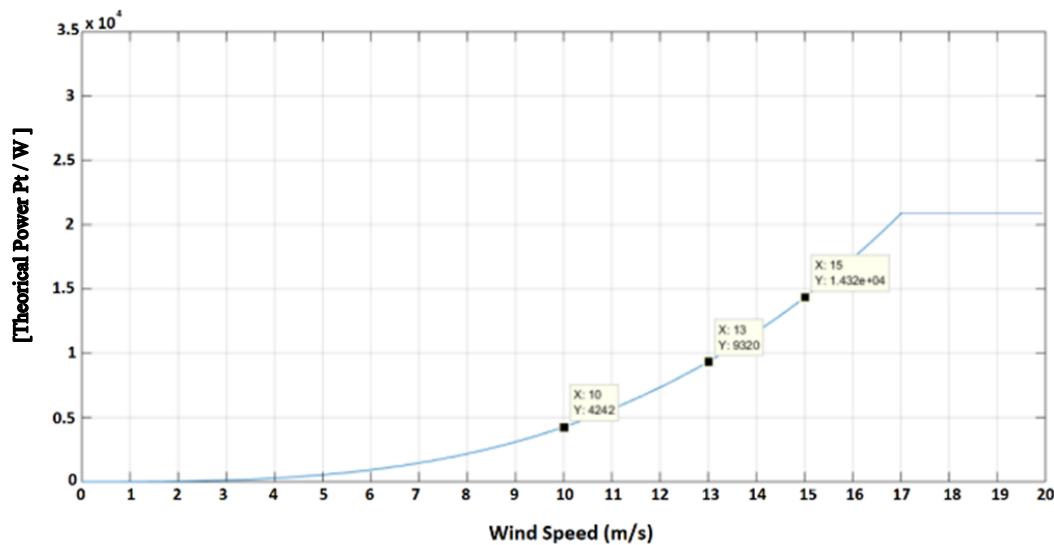The wind turbine power-speed characteristic for the used wind turbine is shown in Fig. 2.

Fig. 2. Wind turbine power-speed characteristic for specific wind turbine analyzed in this study

Fig. 3 is an illustration of the Ct - λ curve for specific wind turbine used in this study.

B. Mechanical Equation of the Wind Turbine and the Shaft

The modeling of the mechanical transmission is as: [11]

$$J\frac{d\omega_m}{dt} = T_t - T_e - \omega_m.f_r \tag{6}$$

where, T_e represents the electromagnetic torque; f_r is the Friction coefficient and J the Wind Turbine Inertia.

Wind turbine and shaft models are represented by Fig. 4.

C. Modeling of the PMSG

In order to facilitate analysis, following assumptions are made:
1. Y-connected stator windings;
2. Excluding eddy current and hysteresis losses;
3. No dynamic response process of excitation current.

Electrical equation of PMSG is expressed as: [9], [14]

$$v_{abc_s} = \frac{d\psi_{abc_s}}{dt} + R_s i_{abc_s} \tag{7}$$

where, v_{abc_s} are the instantaneous a, b, and c 3-ph stator

World Academy of Science, Engineering and Technology
International Journal of Mechanical and Mechatronics Engineering
Vol:14, No:5, 2020

voltages, and i_{abc_s} are the instantaneous 3-ph stator currents. R_s being the stator winding resistance per phase. ψ_{abc_s}, are the instantaneous flux linkages induced by the 3-ph AC currents
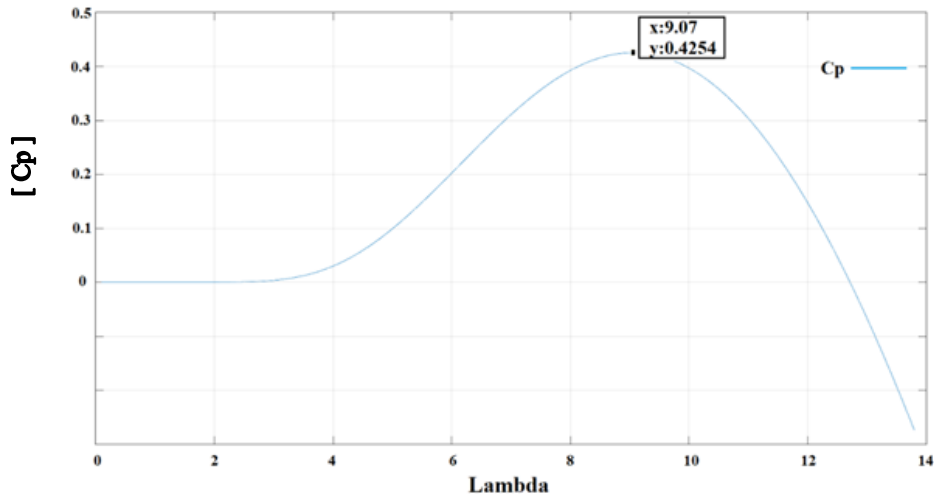
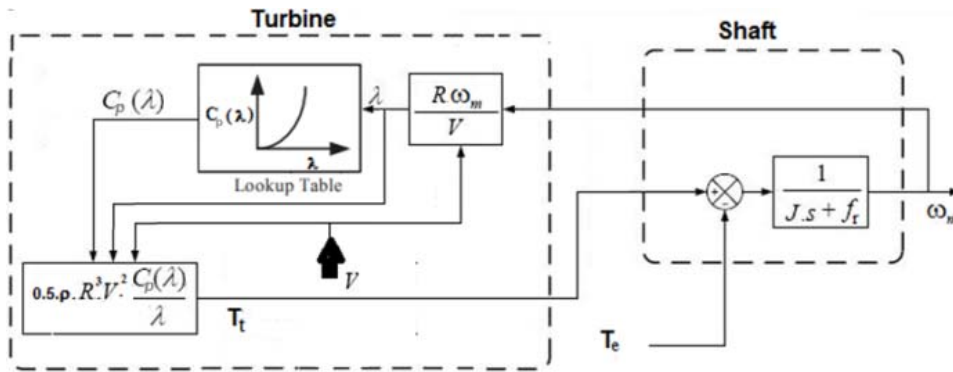and the PM.

Fig. 3 Characteristic function Ct vs. λ

Fig. 4 Wind Turbine and Shaft Models [11]

Applying Park transform, (7) becomes: [15]

$$\begin{bmatrix} v_{d_s} \\ v_{q_s} \end{bmatrix} = [P(\theta_m)][R_s][P(\theta_m)]^{-1} i_{dq_s} +$$
$$[P(\theta_m)][P(\theta_m)]^{-1} \frac{d}{dt}[\psi_{dq_s}] + [P(\theta_m)]\left(\frac{d}{dt}[P(\theta_m)]^{-1}\right)[\psi_{dq_s}] \tag{8}$$

where $P(\theta_m)$ is Park transformation expressed as:

$$P(\theta_m) = \frac{2}{3}\begin{bmatrix} cos(\theta_m) & cos(\theta_m - \frac{2\pi}{3}) & cos(\theta_m + \frac{2\pi}{3}) \\ -sin(\theta_m) & -sin(\theta_m - \frac{2\pi}{3}) & -sin(\theta_m + \frac{2\pi}{3}) \\ \frac{1}{2} & \frac{1}{2} & \frac{1}{2} \end{bmatrix} \tag{9}$$

θ_m, is the angle between q-axis and the main stator axis with:

$$[\psi_{dq_s}] = \begin{bmatrix} \psi_{d_s} \\ \psi_{q_s} \end{bmatrix} = \begin{bmatrix} L_d & 0 \\ 0 & L_q \end{bmatrix}\begin{bmatrix} i_{d_s} \\ i_{q_s} \end{bmatrix} + \begin{bmatrix} \psi_f \\ 0 \end{bmatrix} \tag{10}$$

ψ_f represents the constant permanent magnet flux linkage. Equation (10) can be rewritten as follows [16]

$$[P(\theta_m)][P(\theta_m)]^{-1}\frac{d}{dt}[\psi_{dq_s}] = \frac{d}{dt}(\theta_m).P(\frac{\pi}{2}).[\psi_{dq_s}] = \omega_s[\psi_{dq_s}]' \tag{11}$$

where:

$$[\psi_{dq_s}]' = \begin{bmatrix} -L_q & 0 \\ 0 & L_d \end{bmatrix}\begin{bmatrix} i_{q_s} \\ i_{d_s} \end{bmatrix} + \begin{bmatrix} 0 \\ \psi_f \end{bmatrix} = \begin{bmatrix} -\psi_{q_s} \\ \psi_{d_s} \end{bmatrix} \tag{12}$$

and:

$$[v_{dq_s}] = [R_s][i_{dq_s}] + \frac{d}{dt}[\psi_{dq_s}] + \omega_s[\psi_{dq_s}]' \tag{13}$$

Replacing (14) in (15), (16) is deduced: [11].

$$\begin{cases} v_{d_s} = -\omega_s.\psi_{q_s} + (R_s + pL_d)i_{d_s} \\ v_{q_s} = \omega_s.\psi_{d_s} + (R_s + pL_q)i_{q_s} \end{cases} \tag{14}$$

ω_s is the basic electrical angular frequency of the PMSG and can be deduced from ω_m as:

World Academy of Science, Engineering and Technology
International Journal of Mechanical and Mechatronics Engineering
Vol:14, No:5, 2020

$$\omega_s = n_p . \omega_m \tag{15}$$

where, n_p is the PMSG pole pairs. ψ_{d_s} and ψ_{q_s} are the stator flux linkages corresponding to d-axis and q-axis respectively. Substituting (10) in (14), (16) is obtained: [13].

$$\begin{cases} v_{d_s} = -\omega_s . L_{q_s} i_{q_s} - \omega_s . (R_s + pL_d) i_{d_s} \\ v_{q_s} = \omega_s . L_{d_s} i_{d_s} + (R_s + pL_q) i_{q_s} + E_s \end{cases} \tag{16}$$

with $E_s = \omega_s \, \psi_f$, L_{d_s} and L_{q_s} are the two phase stator windings self-inductances corresponding to d-axis and q-axis. i_{d_s} and i_{q_s} are the armature currents for d-axis and q-axis respectively. (p) is the differential operator symbol.

In the d-q axis rotation coordinate system, (17) expresses mathematical relationship of the PMSG electromagnetic torque:

$$T_e = \frac{3}{2} n_p [\psi_d i_{q_s} + (L_d - L_q) i_{d_s} i_{q_s}] \tag{17}$$

Further, and according to (18), there is a problem of coupling between d and q axis, represented by the terms $\omega_s . \psi_{d_s}$ and $\omega_s . \psi_{q_s}$. Thus, vector control concept is recommended to overcome this problem of coupling. Two inputs v_{d_s} and v_{q_s} are defined to compensate the cross-coupling terms [17], presented as:

$$\text{Comp1: } L_{q_s} \omega_s i_{q_s} \text{ and Comp2: } -\omega_s . L_{d_s} i_{d_s} + \omega_s . \psi_f \tag{18}$$

Further, in order to simplify controlling electromagnetic torque (T_e), Field Orientation Control (FOC) is opted. This latter is achieved by putting $(i_{d_s} = 0)$.

The expression of the torque presented by (17) is therefore reduced to (19):

$$T_e = \frac{3}{2} n_p \psi_f \, i_{q_s} \tag{19}$$

III. CONTROL STRATEGY OF THE MSC

The purpose of MSC control is to regulate the PMSG torque by controlling rotating speed in order to track maximum power while wind speed changes [9], [11]. Further, the MSC control strategy is based on double closed loop control. The speed control as outer loop control, while the current control as inner loop control as shown later in Fig. 5.

A. Strategy of Wind Speed Control (Outer Loop Control)

In this paper, OTSR control is used. The optimal speed ω_m^* is calculated according to MPPT strategy, which is provided as a reference to the external speed loop.

From Fig. 3, for lambda optimum value (λ_{opt}), $C_t(\lambda)$ is maximal. Thus, for this particular value of λ, the blades angular velocity reference (ω_m^*) can be deduced from (2),

$$\omega_m^* = \frac{\lambda_{opt} . v}{R} \tag{20}$$

B. Strategy of Current Control (Inner Loop Control)

The angular speed reference (ω_m^*) presented in (20) is subtracted to the measured blades angular velocity (ω_m). The error resulted is regulated via a PI controller in order to obtain reference quadrature stator current $(i_{q_s}^*)$. The $(i_{d_s}^*)$ current is set to 0, as presented in Fig. 5

$$\begin{cases} i_{q_s}^* = PI(\omega_m^* - \omega_m) \\ i_{d_s}^* = 0 \end{cases} \tag{21}$$

The two voltages $(v_{d_s}^*)$ and $(v_{q_s}^*)$ which are the inputs of the decoupling bloc as described in (18) are calculated as:

$$\begin{cases} v_{q_s}^* = PI(i_{q_s}^* - i_{q_s}) \\ v_{d_s}^* = PI(i_{d_s}^* - i_{d_s}) \end{cases} \tag{22}$$

where:

$$i_{dq_s} = [P(\theta_m)] \, {}_x i_{abc_s}^* \tag{23}$$

This decoupling bloc described in (16) has as outputs $(u_{d_s}^*)$ and $(u_{q_s}^*)$ which present the direct and quadrature voltage components of the modulating signal $(u_{abc_s}^*)$ used to control the MSC, as expressed in (24):

$$u_{abc_s}^* = [P(\theta_m)]^{-1} {}_x u_{dq_x}^* \tag{24}$$

C. PI Regulators Synthesis

After compensation, (14) becomes

$$\begin{cases} v_{d_s} = L_d \frac{di_{d_s}}{dt} + R_s i_{d_s} \\ v_{q_s} = L_q \frac{di_{q_s}}{dt} + R_s i_{q_s} \end{cases} \tag{25}$$

According to (25), we obtain two separate first-order models in the d-q axis [9], [11] shown as:

$$\frac{i_{d_s}}{v_{d_s}} = \frac{1}{sL_d + R_s} \tag{26}$$

$$\frac{i_{q_s}}{v_{q_s}} = \frac{1}{sL_q + R_s} \tag{27}$$

Therefore, we obtain two similar PI regulators which are used in two independent current loops that one of them controls the q-axis component and the second controls d-component as described in Fig. 5.

IV. GSC CONTROL USING RESONANT CONTROLLER

In this method, no direct park transform is needed. Also, only a simple αβ-PLL can be used in this case, Fig. 6. In the outer loop current control, the d-q components of current references $(i_{dq_g}^*)$ can be also calcutated as described in (28) as shown in Fig. 6:

$$\begin{cases} i_{q_g}^* = PI . (v_{dc}^* - v_{dc}) \\ i_{d_g}^* = 0 \end{cases} \tag{28}$$

World Academy of Science, Engineering and Technology
International Journal of Mechanical and Mechatronics Engineering
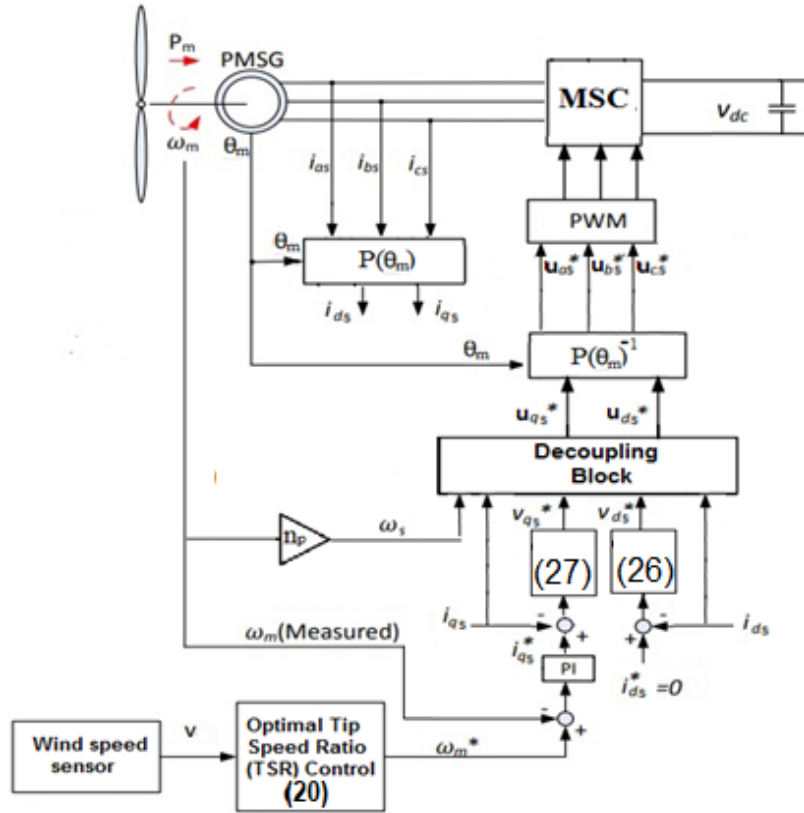Vol:14, No:5, 2020

Fig. 5 Control block diagram of the MSC [9], [11]

Applying Inverse Park transform, the grid currents references in abc coordinate, $(i_{abc_g}^*)$ are deduced in (29)

$$i_{abc_g}^* = \left[P\left(\theta_g \right) \right]^{-1} {}_x i_{dq_g}^* \qquad (29)$$
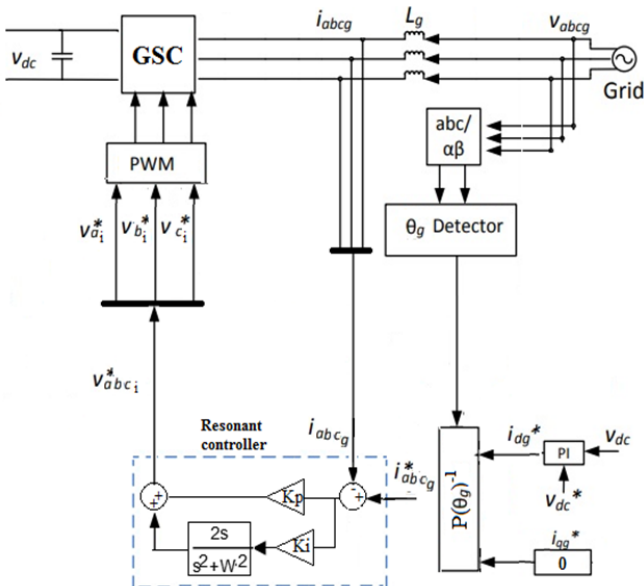
Fig. 6 Block diagram of the proposed GSC Control using resonant controller

From Fig. 6, the deviation between grid currents, (i_{abc_g}) and their references are carried through a resonant regulator [18].

The result is the command of the GSC as expressed in (30):

$$v_{abc_i}^* = (i_{abc_g}^* - i_{abc_g})\left(k_p + k_i . \frac{2s}{s^2 + \omega^2} \right) \qquad (30)$$

k_p, k_i are the proportional and integral coefficients.

We have to point out that with this method the problem of the coupling term is not posed.

V. SIMULATION RESULTS AND ANALYSIS

The wind turbine power-speed characteristic for the used wind turbine is shown in Fig. 2. Fig. 3 illustrates the Ct - λ curve for specific wind turbine used in this study

In order to verify the system characteristics of maintaining stable operation, a scenario of wind speed changes is presented as shown in Fig. 7. The simulation time is set to 3 sec.
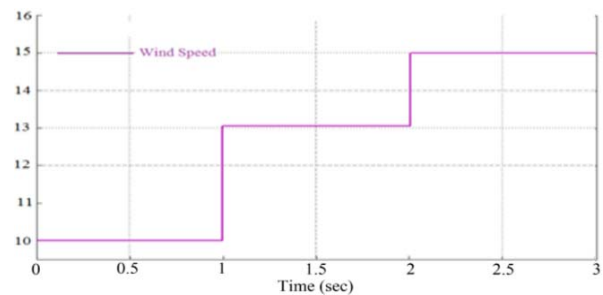

Fig. 7 Scenarios of wind speed

World Academy of Science, Engineering and Technology
International Journal of Mechanical and Mechatronics Engineering
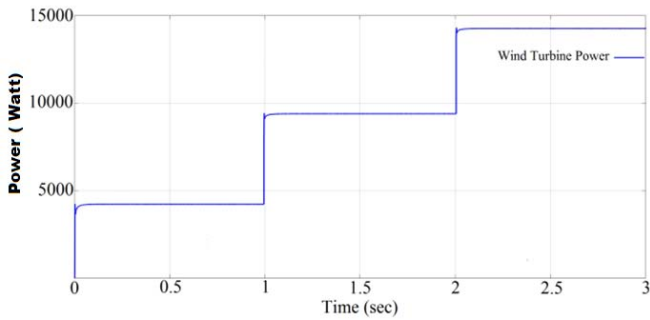Vol:14, No:5, 2020

Fig. 8 Wind turbine Power at different wind speed (10 m/s, 13 m/s, 15 m/s)

Fig. 8 shows that the PMSG based wind turbine has succeeded to track the maximum power curve, which is presented in Fig. 2. Thus, the proposed MPPT controller does its job as it should be.
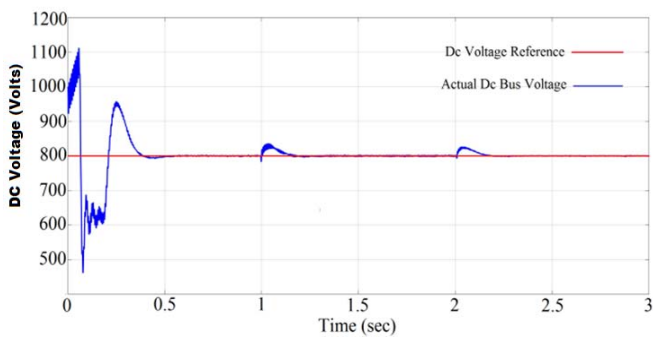

Fig. 9 DC Voltage Reference vs Actual DC Bus Voltage

Fig. 9 shows that the DC-link voltage is maintained constant and follows accurately the reference value as it should be. It is also noticed that DC voltage is well controlled with stabilizing performance and low fluctuation (being about 2,5%).
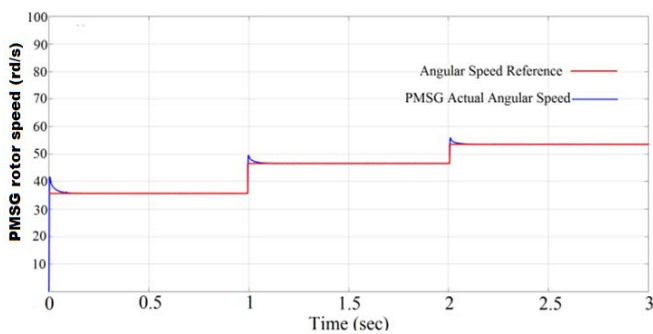

Fig. 10 Angular Speed Reference Vs PMSG rotor Speed

From Fig. 10, in each period [0-1s; 1-2s; 2-3s], the PMSG rotor speed increases to reach the reference value (ω_m^*) as calculated from (22). This simulation result is expected because wind speed is proportional to the active power already discussed in Fig. 8.

Fig. 11 shows that with the increase of the wind speed, currents injected to grid are increased as it should be. It is

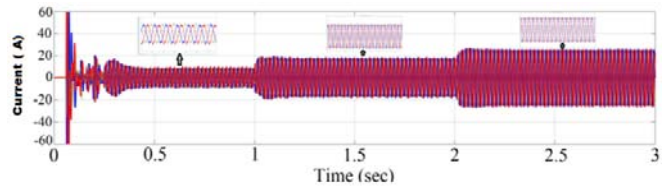noticed that these currents are quite "noisy," which is to be expected when using PWM inverters.

Fig. 11 Waveforms of the 3-ph current injected to the grid
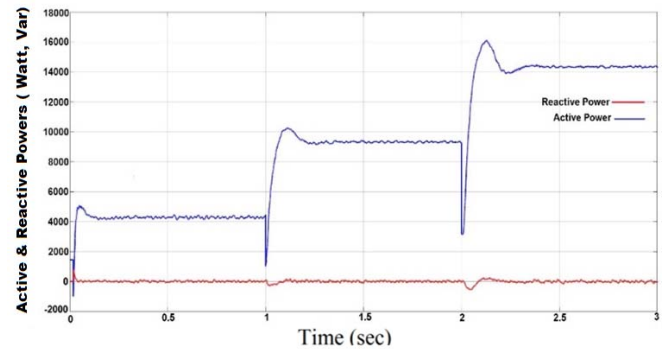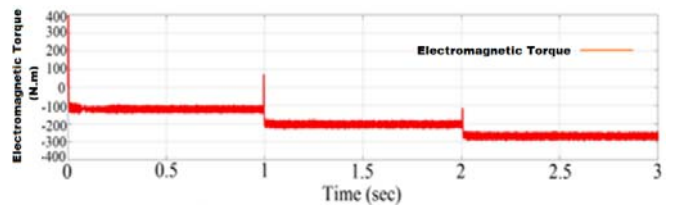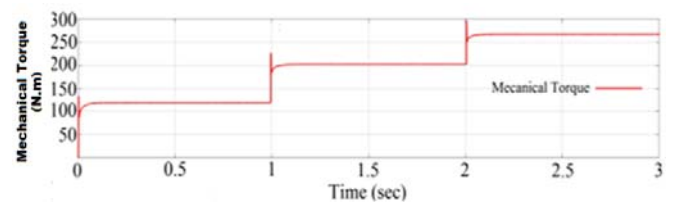

Fig. 12 Active and Reactive Powers delivered by 3-ph VSI

(a)

(b)

Fig. 13 Electromagnetic Torque vs Mechanical Torque

With the increase of the wind speed (as shown in Fig. 7), Figs. 12 and 13 show respectively that generated active power (P), electromagnetic torque (T_e) and mechanical torque (T_t) are gradually increased to their actual values as it should be.

As for the current waveforms presented in Fig. 11, the noise introduced by the PWM inverter is also observed in the electromagnetic torque waveform (Te) shown in Fig. 13 (a). However, the PMSG's inertia prevents this noise from appearing in the PMSG's mecanical torque and speed waveforms as shown in Figs. 13 (b) and 10.

Again, the reason that the actual electrical power generated by the PMSG presented in Fig. 12 is slightly lower than the mechanical power input presented in Fig. 8 is due to the

internal power losses. Thus, conclusions can be made that the control objective was achieved for the studied system under the chosen condition of wind profile.

Finally we can conclude that: The GSC and MSC controllers show their efficiency when simulated under MATLAB/Simulink.

VI. CONCLUSION

Through this paper, the small sized direct-drive PMSG based wind system and connected to grid is developed and analyzed. The wind power system model is built under MATLAB/Simulink using the back-to-back based PECs topology. On the other hand, the simulation results show that when the wind speed decreases or increases, the currents injected into the grid, the PMSG speed and the electromagnetic torque decrease or increase accordingly. The accuracy of the MPPT controller is then demonstrated. Further, through the same simulation results and the same circumstance of wind speed changes, the output active power is stable and the PMSG based wind turbine can be operated in high efficiency as expected. The robustness of the decoupled PQ control to regulate the injected active power into the grid and to achieve a unity power factor is then demonstrated. Also, The DC Bus voltage which is a critical parameter to determine if WECS can incorporate into the power grid is maintained constant even fast variation of wind speed. Thus, the performance of the proposed DC bus voltage control is also verified.

Concerning the use of resonant controller instead of PI controller, results show that it has a higher performance than the PI controller. Indeed, its main role is to follow a sinusoidal reference without having to increase the switching frequency or to adopt a high gain as in the case of the conventional PI controller.

REFERENCES

[1] Yaramasu, V., Wu, B.: 'Model predictive control of wind energy conversion systems' (Wiley-IEEE Press, Hoboken, NJ, 2016, 1st edn.)
[2] Yaramasu, V., Wu, B., Sen, P.C., et al.: 'High-power wind energy conversion systems: state-of-the-art and emerging technologies', Proc. IEEE, 2015, 103, (5), pp. 740–788.
[3] Zhang, Z., Wang, F., Wang, J., Rodríguez, J., & Kennel, R. (2017). Nonlinear direct control for three-level NPC back-to-back converter PMSG wind turbine systems: experimental assessment with FPGA. IEEE Transactions on Industrial Informatics, 13(3), 1172-1183.
[4] Li, S.; Haskew, T. A.; Muljadi, E. & Serrentino, C. (2009). Characteristic Study of Vector-Controlled Direct-Driven Permanent Magnet Synchronous Generator In Wind Power Generation. Electric Power Components and Systems, Vol. 37, No. 10, pp. 1162-1179.
[5] Zhang, J., Cheng, M., Chen, Z., & Fu, X. (2008, April). Pitch angle control for variable speed wind turbines. In Electric Utility Deregulation and Restructuring and Power Technologies, 2008. DRPT 2008. Third International Conference on (pp. 2691-2696). IEEE.
[6] Li, N., Bing, Y. U., Liu, L., & Kong, B. (2014). Simulation study on permanent magnet wind power generation system based on PSIM. SIMULATION,3(4).
[7] Babu, N. R., & Arulmozhivarman, P. (2013). Wind energy conversion systems-a technical review. J. Eng. Sci. Technol, 8(4), 493-507.
[8] Senthilnathan, K., & Annapoorani, K. I. (2016). A review on back-to-back converters in permanent magnet synchronous generator based wind energy conversion system. Indonesian Journal of Electrical Engineering and Computer Science, 2(3), 583-591.
[9] Huang, N. (2013). Simulation of power control of a wind turbine permanent magnet synchronous generator system.
[10] Jena, N. K., Mohanty, K. B., Pradhan, H., & Sanyal, S. K. (2015, June). A decoupled control strategy for a grid connected direct-drive PMSG based variable speed wind turbine system. In Energy, Power and Environment: Towards Sustainable Growth (ICEPE), 2015 International Conference on (pp. 1-6). IEEE.
[11] Elbeji, O., Hamed, M. B., & Sbita, L. (2014). PMSG Wind Energy Conversion System: Modeling and Control. International Journal of Modern Nonlinear Theory and Application, 3(03), 88.
[12] Molina, M. G., & Mercado, P. E. (2008, August). A new control strategy of variable speed wind turbine generator for three-phase grid-connected applications. In Transmission and Distribution Conference and Exposition: Latin America, 2008 IEEE/PES (pp. 1-8). IEEE.
[13] Molina, M. G., & Mercado, P. E. (2011). Modelling and control design of pitch-controlled variable speed wind turbines. In Wind turbines. InTech.
[14] Wang, C. N., Lin, W. C., & Le, X. K. (2014). Modelling of a PMSG wind turbine with autonomous control. Mathematical Problems in Engineering, 2014.
[15] Singh, A. K., Krisham, R., & Sood, Y. (2013). Modeling and control of grid connected variable speed PMSG based wind energy system. In Conference on Advances in Communication and Control Systems 2013 (CAC2S 2013), Published by Atlantis Press.
[16] Kaddouri, A. (2000). Etude d'une commande non-linéaire adaptative d'une machine synchrone à aimants permanents. Université Laval.
[17] Freire, N., Estima, J., & Cardoso, A. (2012). A comparative analysis of PMSG drives based on vector control and direct control techniques for wind turbine applications. Przegląd Elektrotechniczny, 88(1), 184-187.
[18] Mehrasa, M., Pouresmaeil, E., Pournazarian, B., Sepehr, A., Marzband, M., & Catalão, J. (2018). Synchronous Resonant Control Technique to Address Power Grid Instability Problems Due to High Renewables Penetration. Energies, 11(9), 2469.